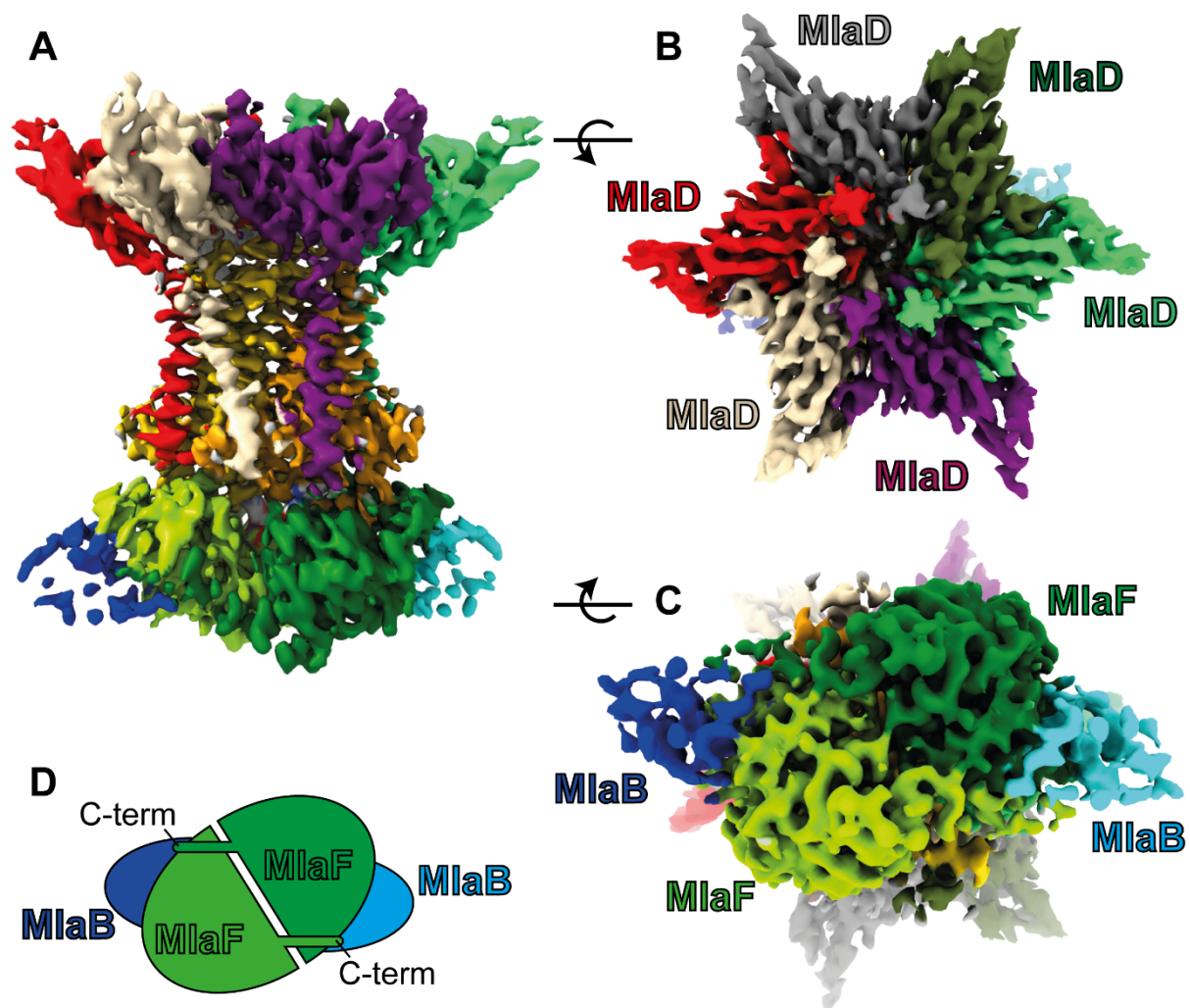


369

370 **Supplemental Figure 1:** processing of the MlaBDEF-AppNHp dataset. Patch motion
 371 correction resulted in a detected defocus range of -1 to -2.5 μm . Initial blob picking with a
 372 diameter range from 120-150 \AA including elliptical shapes were extracted and 2D classified
 373 two times into each 250 classes. Ab initio 3D models were generated and the best class was
 374 used to re-pick particles template-based. After two rounds of 2D classification an ab initio 3D
 375 model was generated and refined using CryoSPARC's Non-Uniform (NU) refinement
 376 procedure with C2 symmetry, followed by global and local CTF refinement and two rounds of
 377 ab initio model generation with class similarity values of 0.1 and 0.5, respectively. The final
 378 particle stack contained 93.295 particles and was NU refined to 3.92 \AA with C2 symmetry
 379 (4.07 \AA with C1 symmetry). The map was sharpened with the Guinier plot B-factor of -200 \AA
 380 ². Fourier Shell Correlation plot is indicated as well as local resolutions at FSC=0.5 projected
 381 on the final map. A histogram with the full local resolution range is also indicated. The first
 382 high resolution 3D structure was used as an input for CryoSPARC's 3D variability jobtype
 383 with 6 modes. Only the first three modes showed global changes; firstly, translation of MlaD
 384 against MlaBEF (Supplemental Movie 1), secondly, rotation of the MlaBEF part against MlaD
 385 (Supplemental Movie 2) and thirdly, alternating appearance of MlaB, indicating lower
 386 occupancy of this part compared to the MlaDEF part.

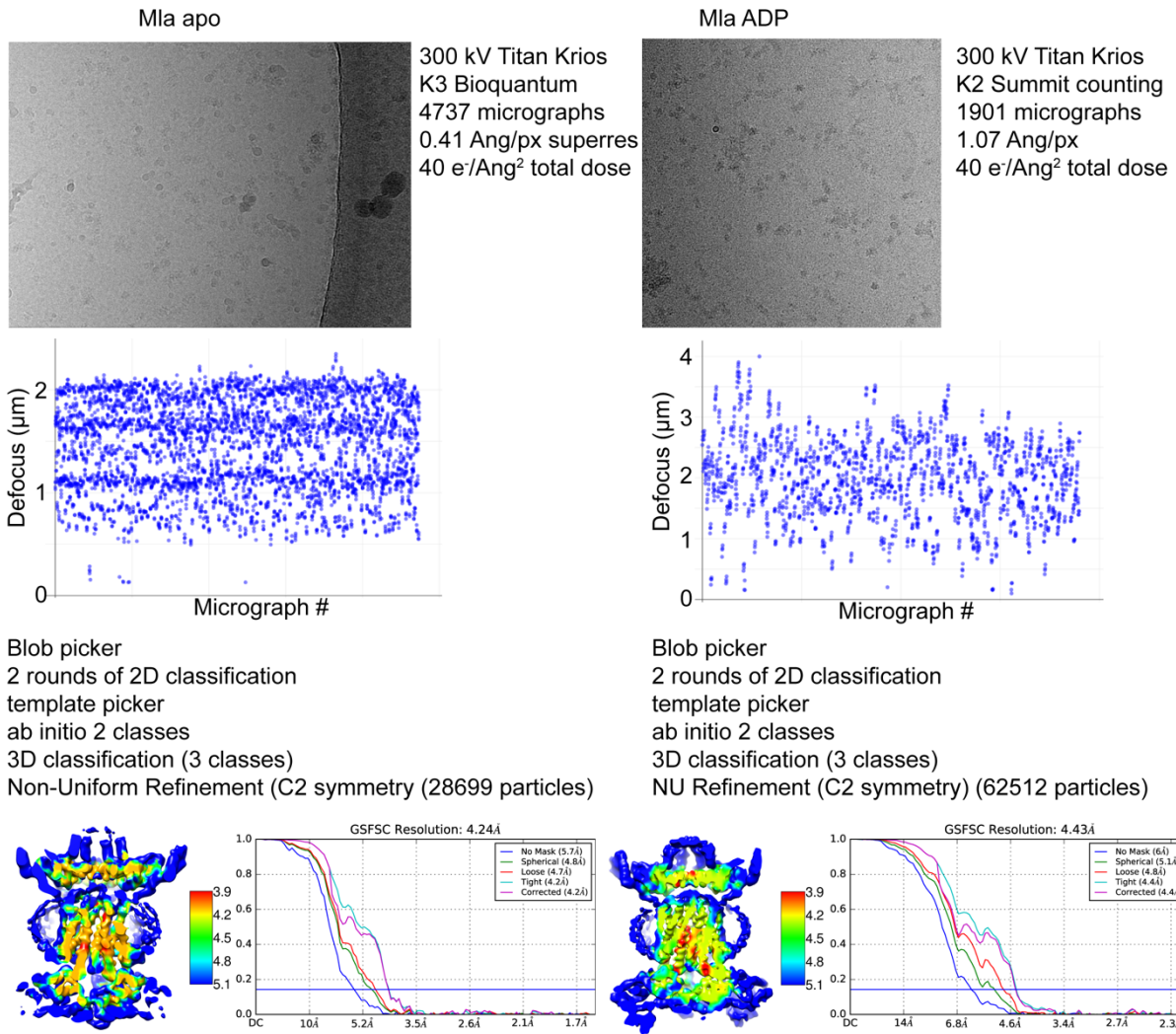
387



388

389 **Supplemental Figure 2:** Side (A), top (B) and bottom (C) views of MlaBDEF. The MlaBFFB
 390 tetramer is stabilized by a “handshake mechanism” (D). C-terminal regions of MlaF bind the
 391 opposing MlaB subunit.

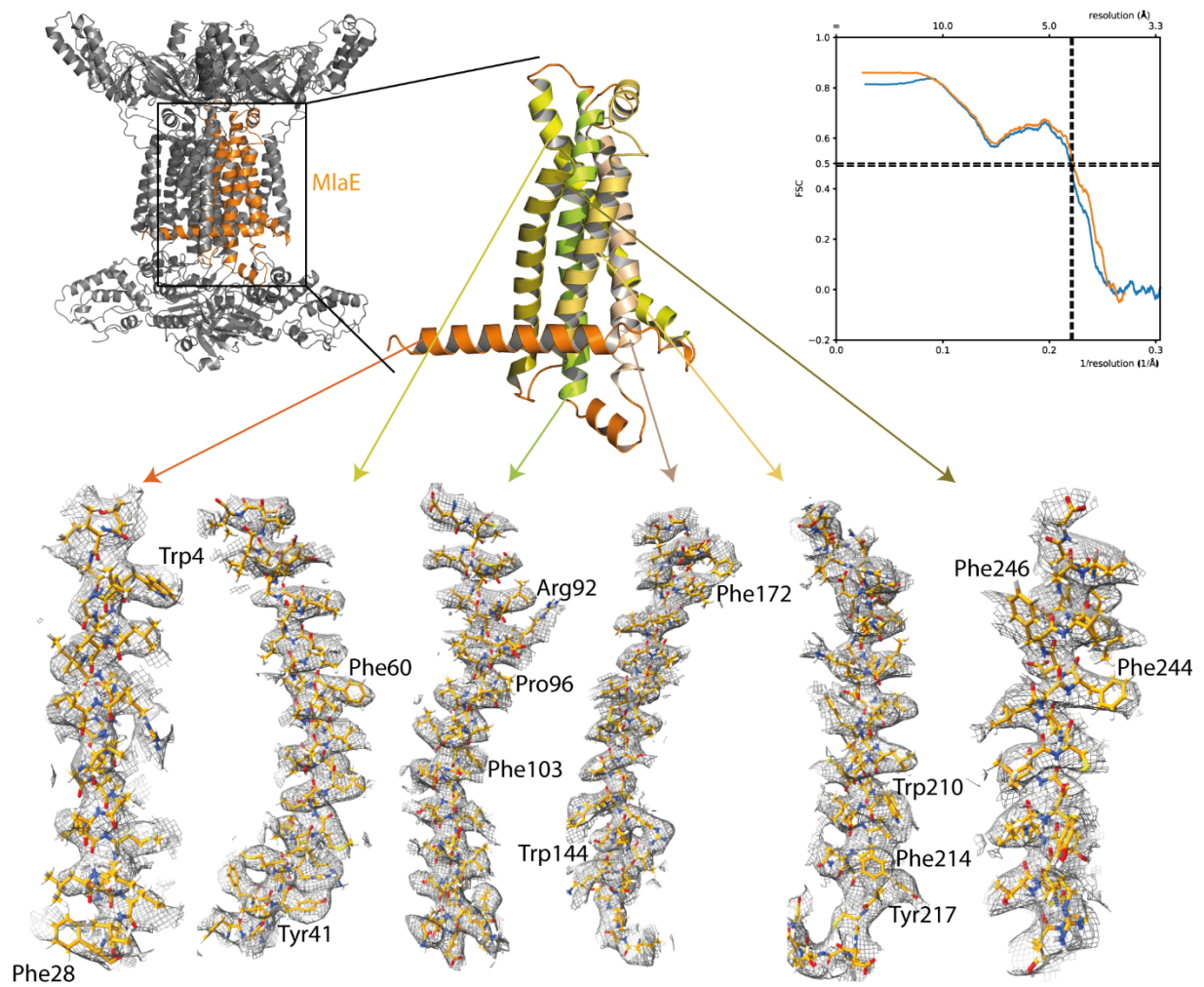
392



393

394 **Supplemental Figure 3:** processing of the MlaBDEF-ADP and MlaBDEF apo datasets in
 395 After blob picking and 2D classification selected 2D classes were used for template picking.
 396 After several rounds of ab initio 3D structure generation and 3D classification Non-uniform
 397 refinement in C2 symmetry resulted in slightly lower resolutions compared to MlaBDEF-
 398 AppNHp. Global and local CTF refinement did not increase the map resolution.

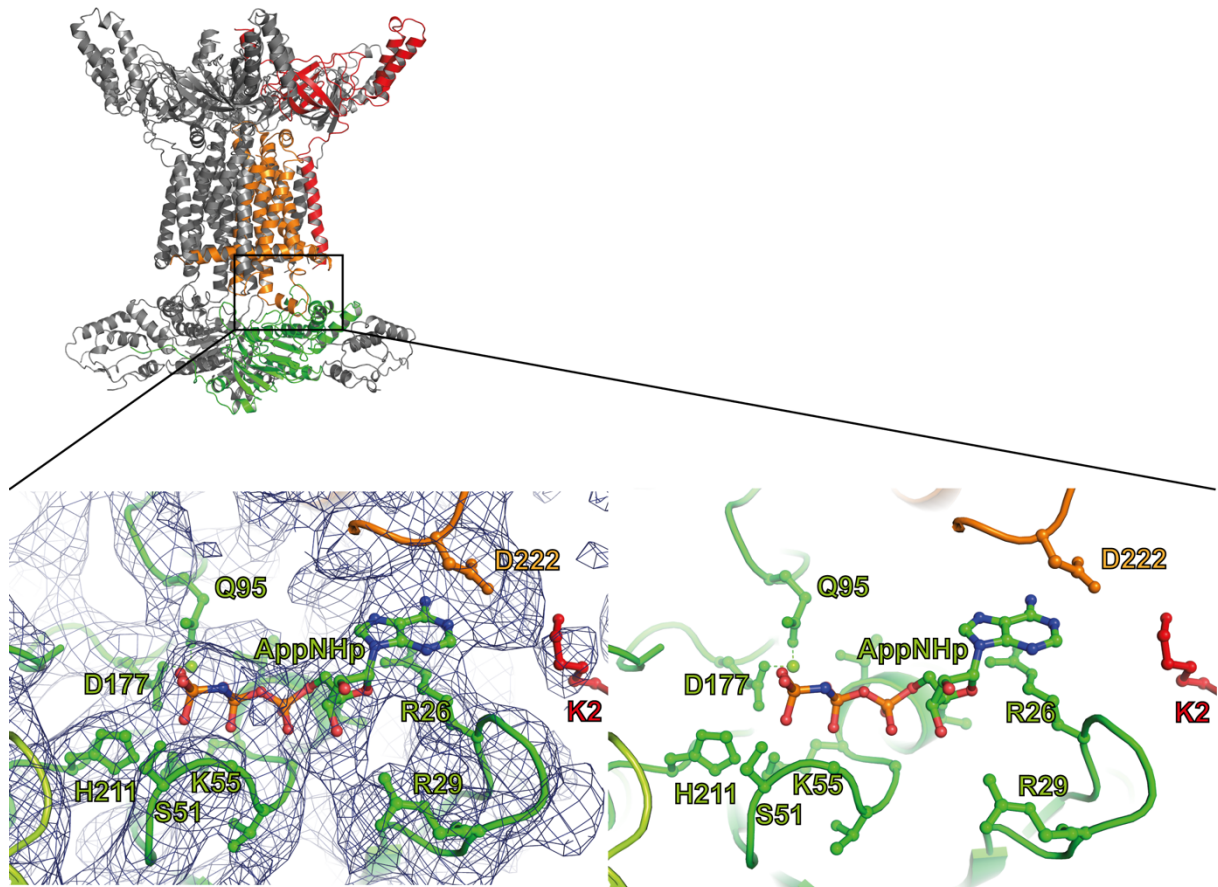
399



400

401 **Supplemental Figure 4:** de novo model building of MlaE (orange). Large side chains that
 402 allowed sequence mapping are indicated as well as map to model FSC of the whole
 403 MlaBDEF protein complex to the AppNHp map.

404

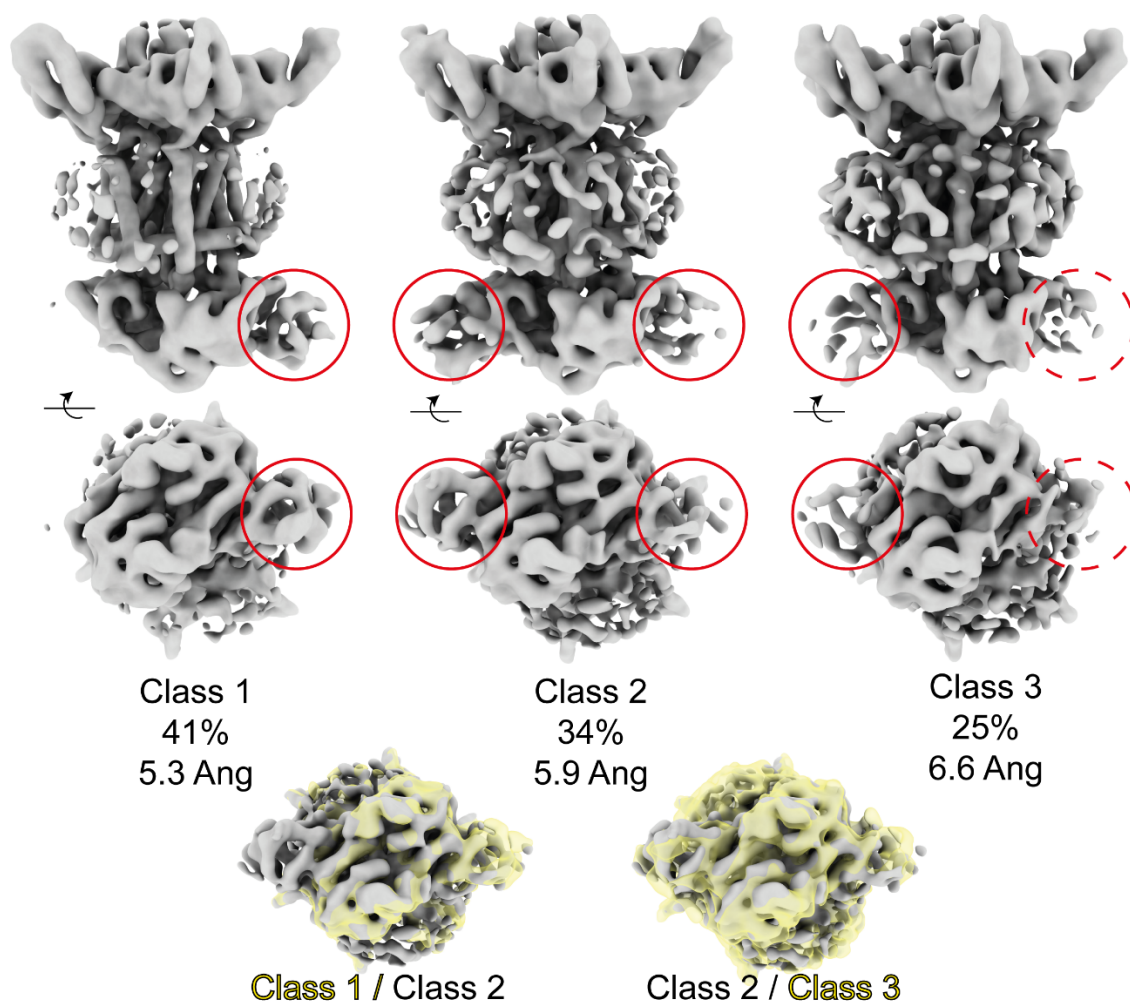


405

406 **Supplemental Figure 5:** AppNhp is bound at the interface of MlaE (orange), MlaD (red) and
407 MlaF (green).

408

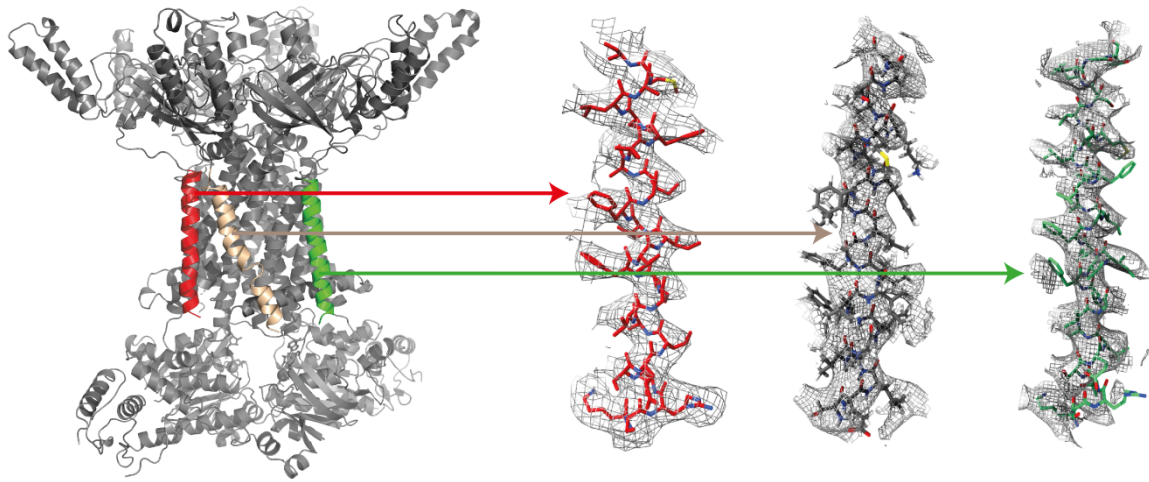
409



410

411 **Supplemental Figure 6:** MlaB binding (red circles) occurred on both binding sites in about
 412 50% of the particles (classes 2 and 3) and on only one binding site in the other 50% of the
 413 particles (class 1). Maps were obtained by Non-Uniform refinement in C1 symmetry after
 414 heterogeneous refinement with 3 classes in CryoSPARC. Alignments of Classes 1-3 show
 415 no major structural changes upon MlaB binding.

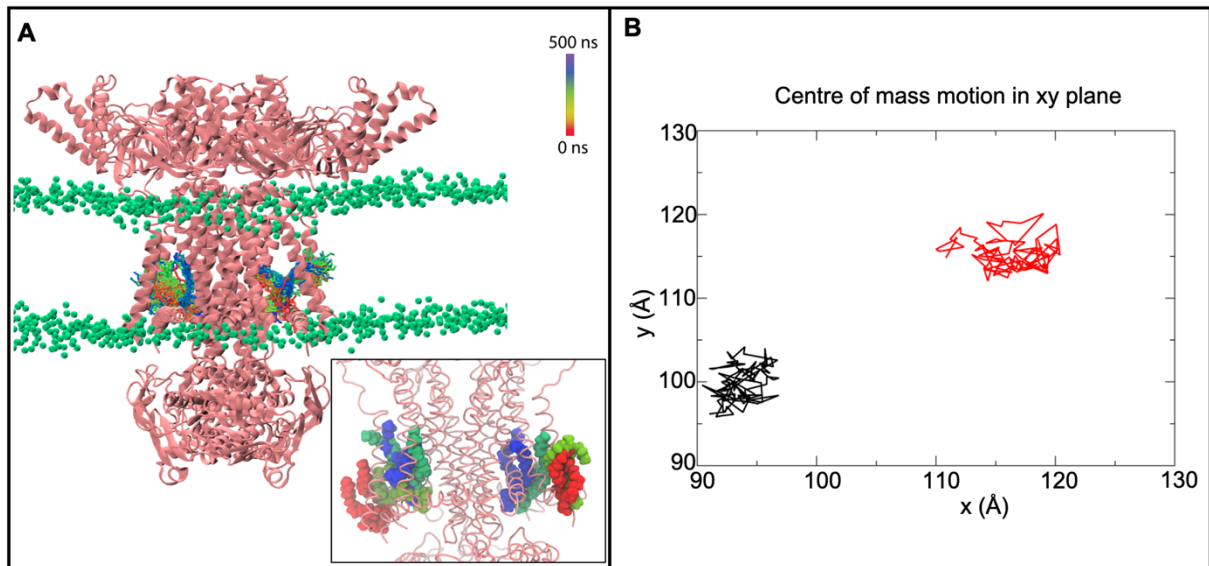
416



417

418 **Supplemental Figure 7:** Enclosed N-Helix of MlaD is significantly better resolved compared
419 to peripheral MlaD N-helices (grey, green).

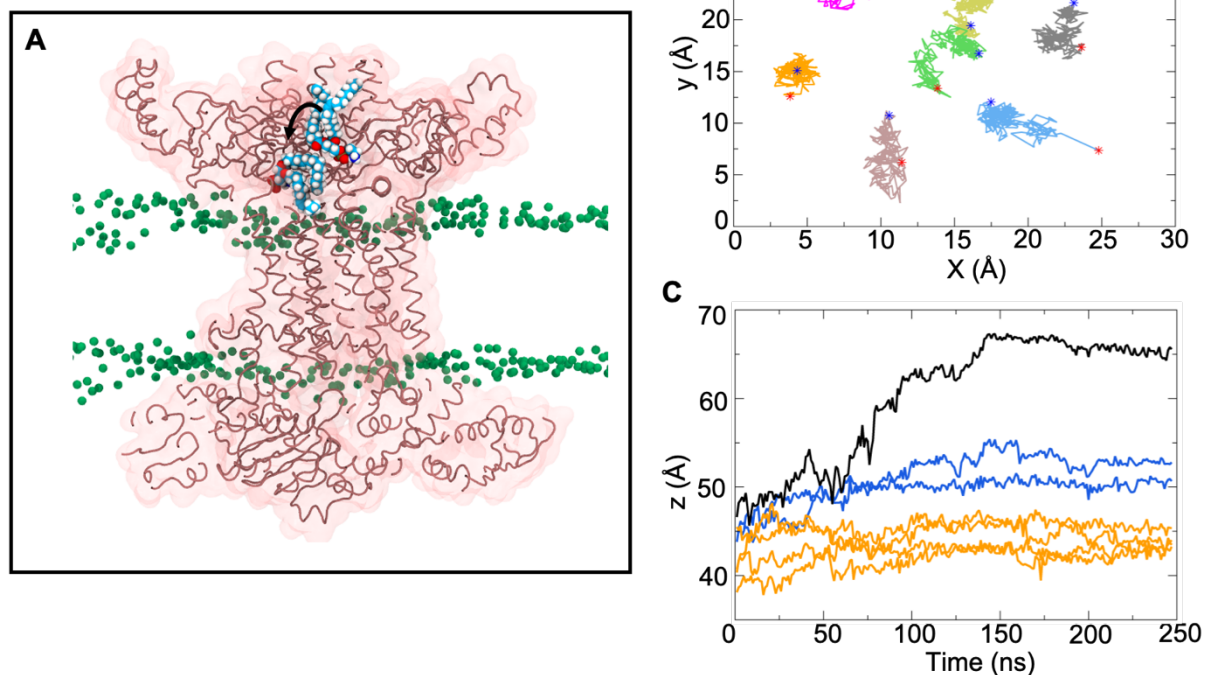
420



421

422 **Supplemental Figure 8:** Panel A shows the location of two POPE lipids during a 500 ns
 423 simulation, the colour scheme indicates the movement of the lipids as shown in the legend. In
 424 this simulation the lipids moved into this location spontaneously during the equilibration
 425 process, as shown in the close-up view in the inset in which the red coloured lipids indicate
 426 positions lipid positions at the start of the equilibration process. Panel B shows the motion of
 427 the lipids in the xy plane over 500 ns. The lipids are confined within an area of 10 x 10 Å for
 428 500 ns, showing this location is favourable.

429



430

431 **Supplemental Figure 9:** Panel A shows a cut-away view of the protein with a POPE lipid at
 432 two time points during the simulation, time = 0 ns and 150 ns. The Mla_{7PE} simulation was
 433 initiated with seven POPE lipids placed at the periplasmic end of the protein corresponding to
 434 the density for detergents in the cryo-EM data (Table S2). The lipid which is displaced more
 435 towards the cytoplasmic end is from the frame at t = 150 ns. The central hydrophobic ‘channel’
 436 of the protein is a clear conduit for lipids given the spontaneous movement of POPE into this
 437 region in just 150 ns. Panel B shows the center of mass motion of the seven lipids in the xy
 438 plane. They are confined to an area of ~5 x 5 Å, indicating this is a high lipid affinity region.
 439 Panel C shows the center of mass movement of the seven lipids in the Z dimension as a
 440 function of time. The higher values of z correspond to the cytoplasmic end of the protein. The
 441 lipid shown in panel A corresponds to the black curve showing a clear movement towards the
 442 cytoplasmic end. Three other lipids (blue) move into this channel but to a lesser extent than
 443 the aforementioned lipid, whereas three others (orange) remain close to their starting positions.
 444 It is important to note that the simulations from a model at the reported resolution do not really
 445 tell us about the directionality of the movement, but rather that these regions are conduits for
 446 lipids

447

Table S1: cryo-EM data collection, refinement and validation statistics

	AppNHp (EMDB-11082 (PDB: 6Z5U))	Apo (EMDB-11083)	ADP (EMDB-11084)
Data Collection and Processing			
Microscope	Titan Krios	Titan Krios	Titan Krios
Voltage (kV)	300	300	300
Camera	K2 summit	K3 bioquantum	K2 summit
Pixel size (Å)	1.07	0.41	1.07
Defocus range (μm)	-1 to -2.5	-0.8 to -2.0	-1 to -2.5
Total dose (eÅ ⁻²)	47	40	40
Number of micrographs	2557	4737	1901
Total particles used	93,295	28,699	62,512
Map Resolution (Å)	3.92	4.24	4.43
Refinement			
Model composition			
Non-hydrogen atoms	17,892		
Protein Residues	2334		
Ligand atoms	4		
<i>B</i> factors (Å ⁻¹)			
Protein	145.24		
Ligand	170.31		
R.m.s. deviations			
Bond lengths (Å)	0.008		
Bond angles (°)	1.384		
Validation			
MolProbity score	3.43		
Clashscore	35.15		
Poor rotamers (%)	10.94		
Ramachandran plot			
Favoured (%)	87.45		
Allowed (%)	10.94		
Disallowed (%)	0.43		

451

452

453

454 **Table S2: Equilibrium Protocol for MD simulations**

Step	Time Step (fs)	Total Time (ns)	Protein Backbone Restraints ($\text{kJ mol}^{-1} \text{nm}^{-2}$)	Protein Sidechain Restraints ($\text{kJ mol}^{-1} \text{nm}^{-2}$)	Ensemble
1	1	0.125	4000	2000	NVT
2	1	0.125	2000	1000	NVT
3	1	0.125	1000	500	NPT
4	2	0.5	500	200	NPT
5	2	0.5	200	50	NPT
6	2	20	50	0	NPT

455

456

457

458 **Table S3: Summary of the equilibrium MD simulation systems**

System	Additional lipids	Temperature (K)	Simulation Length (ns)
Mla	-	310	500 ($\times 2$)
Mla	-	323	500 ($\times 2$)
Mla_7PE	7 POPE	310	250 ($\times 2$)

459

460